Supporting Information

Nitrogen Trifluoride Complexes of Group 10 Transition Metals $M(NF_3)$ (M= Pd, Pt)

Guohai Deng,*[a] Yan Lu, [a] Tony Stüker, [a] Sebastian Riedel*[a]

[a] Dr. G. H. Deng, Y. Lu, Dr. T. Stüker, Prof. Dr. S. Riedel
Freie Universität Berlin
Institut für Chemie und Biochemie–Anorganische Chemie
Fabeckstrasse 34/36, 14195 Berlin (Germany)
E-mail: ghdeng@zedat.fu-berlin.de, s.riedel@fu-berlin.de

Experimental and Computational Details

The experimental method for matrix isolation infrared spectroscopy has been described in more detail in our previous works.[1] Briefly, the 1064 nm Fundamental of a Nd:YAG laser (Continuum, Minilite II, 10 Hz repetition rate with 10 ns pulse width) with a pulse energy of up to 65-70 mJ cm^{-2} was used to ablate rotating Pd, Pt metal target to form metal atoms. The produced metal atoms were co-deposited with nitrogen trifluoride (0.1%) in excess argon onto a CsI window cooled to 4 K using a closed-cycle helium refrigerator. $^{14}NF_3$ and $^{15}NF_3$ samples were prepared according to published protocols and described elsewhere.[2] After 60 min sample deposition, infrared spectra were recorded on a Bruker Vertex 70 spectrometer purged with dry air at 0.5 cm^{-1} resolution in the region between 4000 and 450 cm^{-1} using a liquid nitrogen cooled mercury cadmium telluride (MCT) detector. The matrix samples were subjected to irradiation with visible light using a LED light (OSLON 80 4+ PowerStar Circular 4 LED Arrays：$\lambda = 470 \pm 20$ nm).

Density functional theory (DFT) calculations were carried out using the Gaussian 16 program package.[3] The hybrid functional B3LYP[4] was performed in our calculations to predict the molecular structures and vibrational frequencies of the experimental observed products. The Coupled Cluster Single Double and perturbative Triple excitations CCSD(T)[5] calculations were carried out in the spin restricted RHF-CCSD(T) close-shell (unrestricted ROHF-UCCSD(T) open-shell) coupled cluster formalism using default frozen core settings as implemented in the Molpro2019 software package.[6] The polarized triplet-ζ plus diffuse functions aug-cc-pVTZ basis set was used for the N and F atoms and the aug-cc-pVTZ-PP valence basis and associated scalar-relativistic pseudopotential (PP) for Pd and Pt.[7]

References

1 T. Schlöder, T. Vent-Schmidt and S. Riedel, *Angew. Chem. Int. Ed.,* 2012, **51**, 12063.

2 T. Stüker, T. Hohmann, H. Beckers and S. Riedel, *Angew. Chem. Int. Ed.,* 2020, **59**, 23174.

3 M. J. Frisch, G. W. Trucks, H. B. Schlegel, G. E. Scuseria, M. A. Robb, J. R. Cheeseman, G. Scalmani, V. Barone, G. A. Petersson, H. Nakatsuji, X. Li, M. Caricato, A. V. Marenich, J. Bloino, B. G. Janesko, R. Gomperts, B. Mennucci, H. P. Hratchian, J. V. Ortiz, A. F. Izmaylov, J. L. Sonnenberg, D. Williams-Young, F. Ding, F. Lipparini, F. Egidi, J. Goings, B. Peng, A. Petrone, T. Henderson, D. Ranasinghe, V. G. Zakrzewski, J. Gao, N. Rega, G. Zheng, W. Liang, M. Hada, M. Ehara, K. Toyota, R. Fukuda, J. Hasegawa, M. Ishida, T.

Nakajima, Y. Honda, O. Kitao, H. Nakai, T. Vreven, K. Throssell, J. A. Montgomery, Jr., J. E. Peralta, F. Ogliaro, M. J. Bearpark, J. J. Heyd, E. N. Brothers, K. N. Kudin, V. N. Staroverov, T. A. Keith, R. Kobayashi, J. Normand, K. Raghavachari, A. P. Rendell, J. C. Burant, S. S. Iyengar, J. Tomasi, M. Cossi, J. M. Millam, M. Klene, C. Adamo, R. Cammi, J. W. Ochterski, R. L. Martin, K. Morokuma, O. Farkas, J. B. Foresman, and D. J. Fox, *Gaussian 16*, Gaussian, Inc., Wallingford CT, 2016.

4 *(a)* P. J. Stephens, F. J. Devlin, C. F. Chabalowski and M. J. Frisch, *J. Phys. Chem.,* 1994, **98**, 11623; *(b)* A. D. Becke, *J. Chem. Phys.,* 1993, **98**, 5648; *(c)* C. Lee, W. Yang and R. G. Parr, *Phys. Rev. B,* 1988, **37**, 785; *(d)* S. H. Vosko, L. Wilk and M. Nusair, *Can. J. Phys.,* 1980, **58**, 1200.

5 *(a)* K. Raghavachari, G. W. Trucks, J. A. Pople and M. Head-Gordon, *Chem. Phys. Lett.,* 1989, **157**, 479; *(b)* G. D. Purvis and R. J. Bartlett, *J. Chem. Phys.,* 1982, **76**, 1910.

6 H.-J. Werner, P. J. Knowles, G. Knizia, F. R. Manby, M. Schütz, P. Celani, W. Györffy, D. Kats, T. Korona, R. Lindh, A. Mitrushenkov, G. Rauhut, K. R. Shamasundar, T. B. Adler, R. D. Amos, S. J. Bennie, A. Bernhardsson, A. Berning, D. L. Cooper, M. J. O. Deegan, A. J. Dobbyn, F. Eckert, E. Goll, C. Hampel, A. Hesselmann, G. Hetzer, T. Hrenar, G. Jansen, C. Köppl, S. J. R. Lee, Y. Liu, A. W. Lloyd, Q. Ma, R. A. Mata, A. J. May, S. J. McNicholas, W. Meyer, T. F. Miller III, M. E. Mura, A. Nicklass, D. P. O'Neill, P. Palmieri, D. Peng, K. Pflüger, R. Pitzer, M. Reiher, T. Shiozaki, H. Stoll, A. J. Stone, R. Tarroni, T. Thorsteinsson, M. Wang and M. Welborn, *MOLPRO, version 2019.2, a package of ab initio programs*.

7 *(a)* D. Figgen, K. A. Peterson, M. Dolg and H. Stoll, *J. Chem. Phys.,* 2009, **130**, 164108; *(b)* K. A. Peterson, D. Figgen, M. Dolg and H. Stoll, *J. Chem. Phys.,* 2007, **126**, 124101; *(c)* R. A. Kendall, T. H. Dunning and R. J. Harrison, *J. Chem. Phys.,* 1992, **96**, 6796.

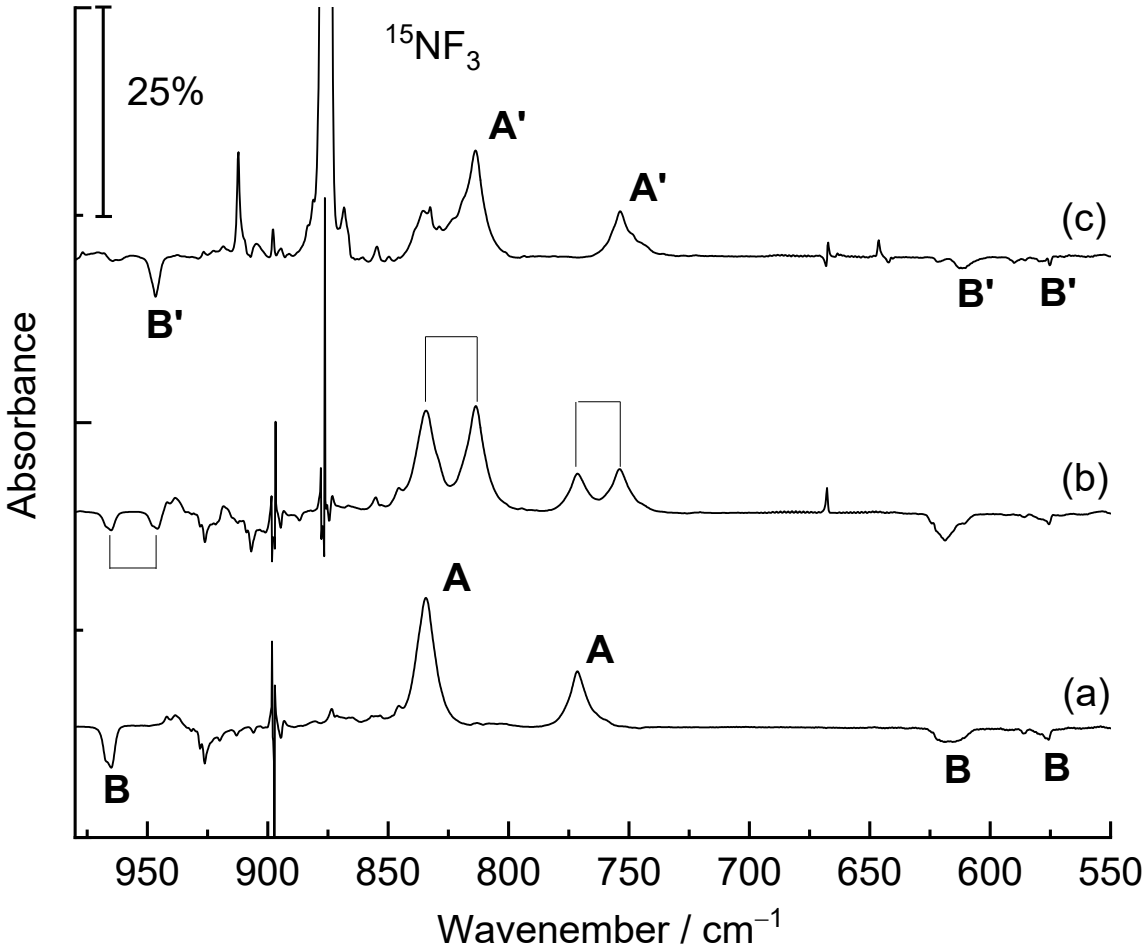

Fig. S1. Difference infrared spectra in the 980-550 cm^{-1} region from co-deposition of Pd atoms with nitrogen trifluoride in solid argon and recorded after 10 min of blue LED (λ = 470 nm) light irradiation minus the spectra recorded after annealing to 20 K. (a) Pd + 0.1% $^{14}NF_3$; (b) Pd + 0.1% $^{14}NF_3$ + 0.1% $^{15}NF_3$; (c) Pd + 0.1% $^{15}NF_3$. **A**: Pd($^{14}NF_3$); **B**: F^{14}NPdF$_2$; **A'**: Pd($^{15}NF_3$); **B'**: F^{15}NPdF$_2$.

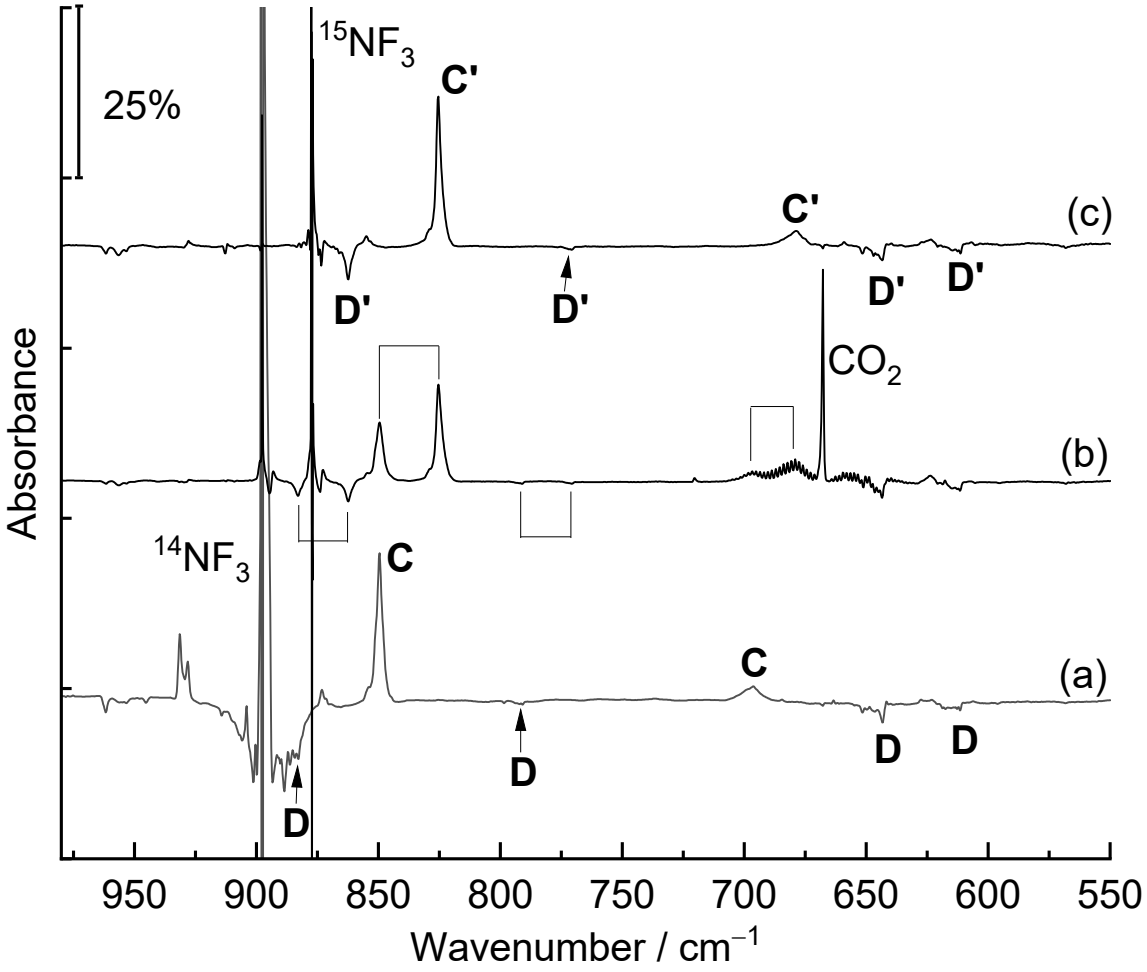

Fig. S2. Difference infrared spectra in the 980-550 cm^{-1} region from co-deposition of Pt atoms with nitrogen trifluoride in solid argon and recorded after 10 min of blue LED (λ = 470 nm) light irradiation minus the spectra recorded after annealing to 20 K. (a) Pt + 0.1% $^{14}NF_3$; (b) Pt + 0.1% $^{14}NF_3$ + 0.1% $^{15}NF_3$; (c) Pt + 0.1% $^{15}NF_3$. **C**: Pt($^{14}NF_3$); **D**: F^{14}NPtF$_2$; **C'**: Pt($^{15}NF_3$); **D'**: F^{15}NPtF$_2$.

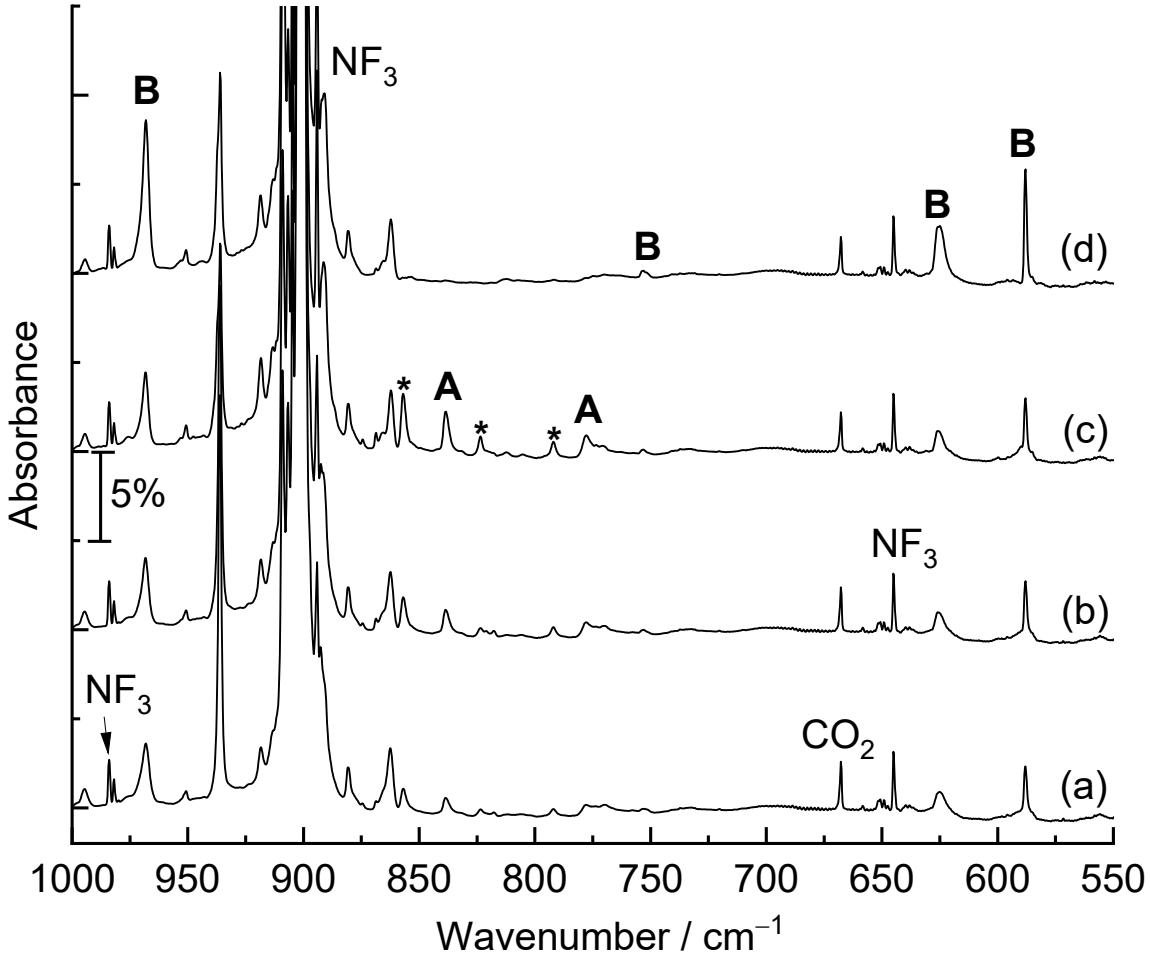

Fig. S3. Infrared spectra in the 1000–550 cm^{-1} region from co-deposition of laser-ablated Pd atoms with 0.1% NF_3 in neon. (a) After 60 min of sample deposition, (b) after annealing to 8 K, (c) after annealing to 10 K, (d) after 10 min of blue LED (λ = 470 nm) light irradiation. **A**: $Pd(NF_3)$; **B**: $FNPdF_2$. Unknown species are marked by asterisks.

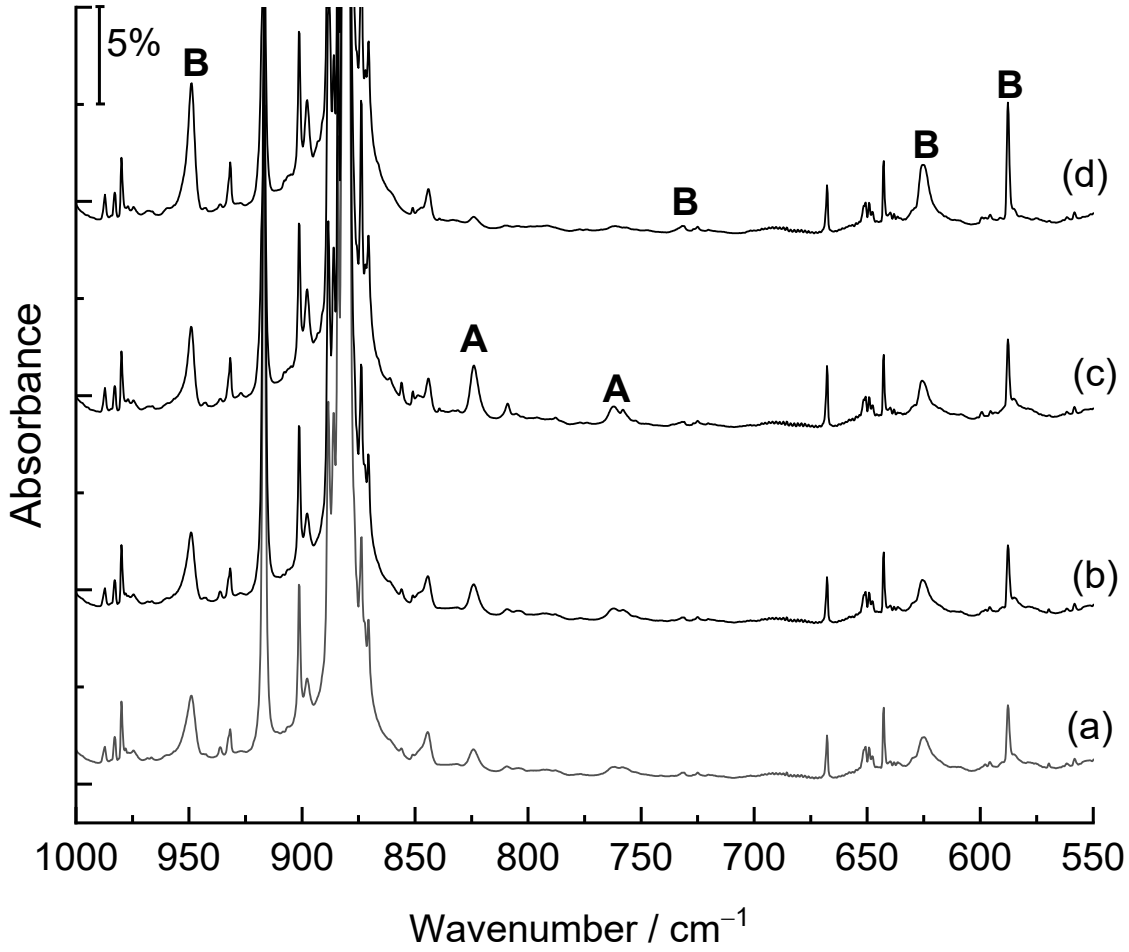

Fig. S4. Infrared spectra in the 1000–550 cm^{-1} region from co-deposition of laser-ablated Pd atoms with 0.1% $^{15}NF_3$ in neon. (a) After 60 min of sample deposition, (b) after annealing to 8 K, (c) after annealing to 10 K, (d) after 10 min of blue LED (λ = 470 nm) light irradiation. **A**: Pd($^{15}NF_3$); **B**: F^{15}NPdF_2.

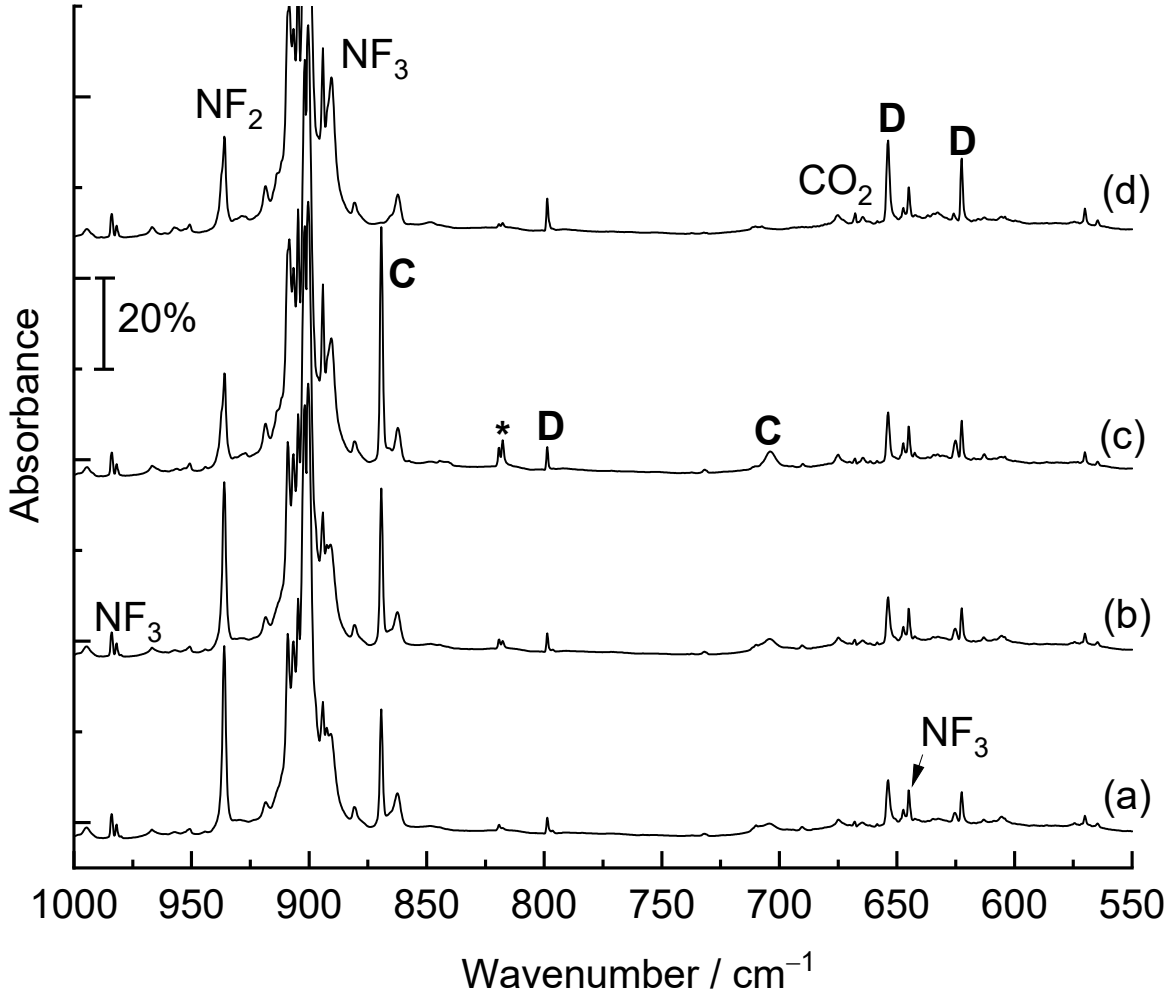

Fig. S5. Infrared spectra in the 1000–550 cm^{-1} region from co-deposition of laser-ablated Pt atoms with 0.1% NF_3 in neon. (a) After 60 min of sample deposition, (b) after annealing to 8 K, (c) after annealing to 10 K, (d) after 10 min of blue LED (λ = 470 nm) light irradiation. **C**: $Pt(NF_3)$; **D**: $FNPtF_2$. Unknown species are marked by an asterisk.

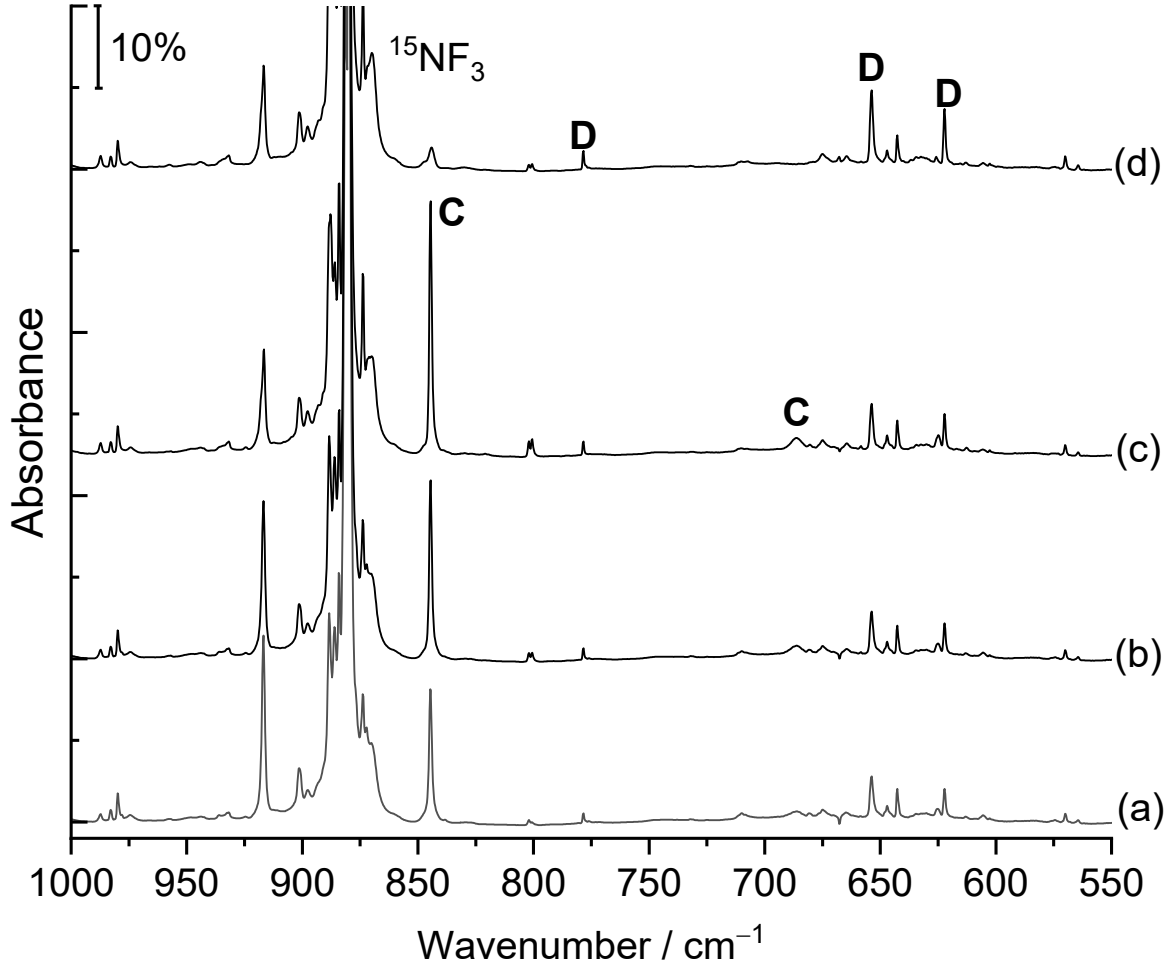

Fig. S6. Infrared spectra in the 1000–550 cm^{-1} region from co-deposition of laser-ablated Pt atoms with 0.1% $^{15}NF_3$ in neon. (a) After 60 min of sample deposition, (b) after annealing to 8 K, (c) after annealing to 10 K, (d) after 10 min of blue LED (λ = 470 nm) light irradiation. **C**: Pt($^{15}NF_3$); **D**: F^{15}NPtF$_2$.

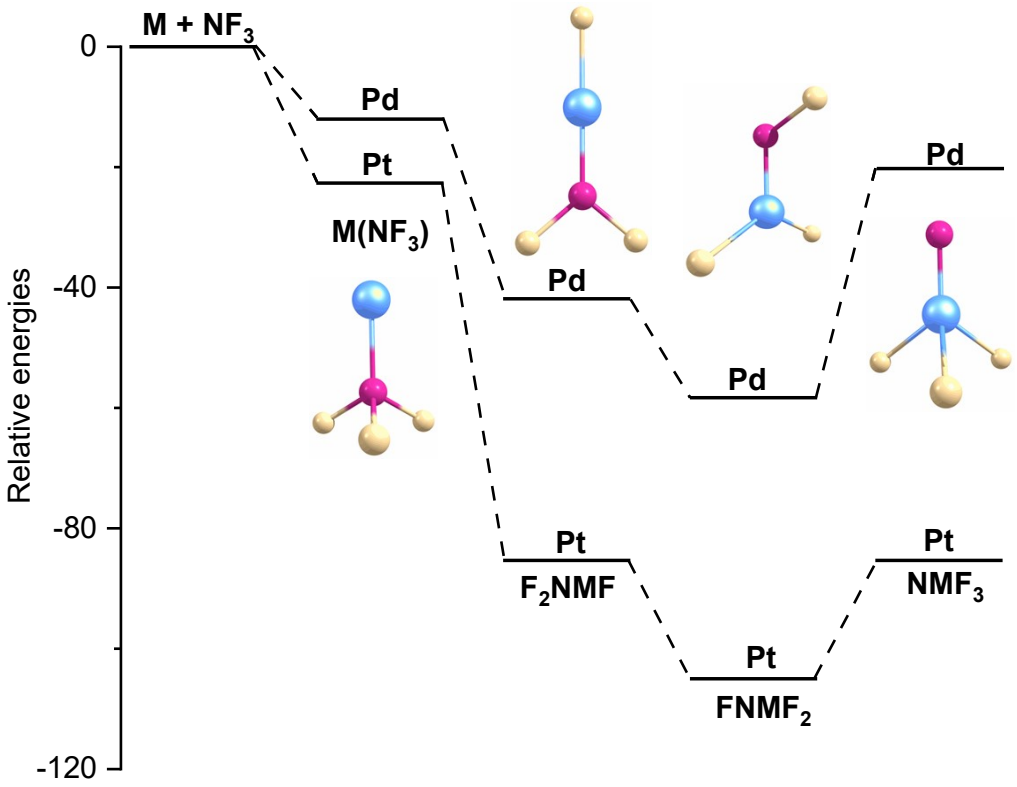

Fig. S7. Calculated energies of the plausible products in relation to the precursors metal atoms M (M = Pd, Pt) and NF_3 at B3LYP/aug-cc-pVTZ-(pp) level. The energies are in kcal/mol.

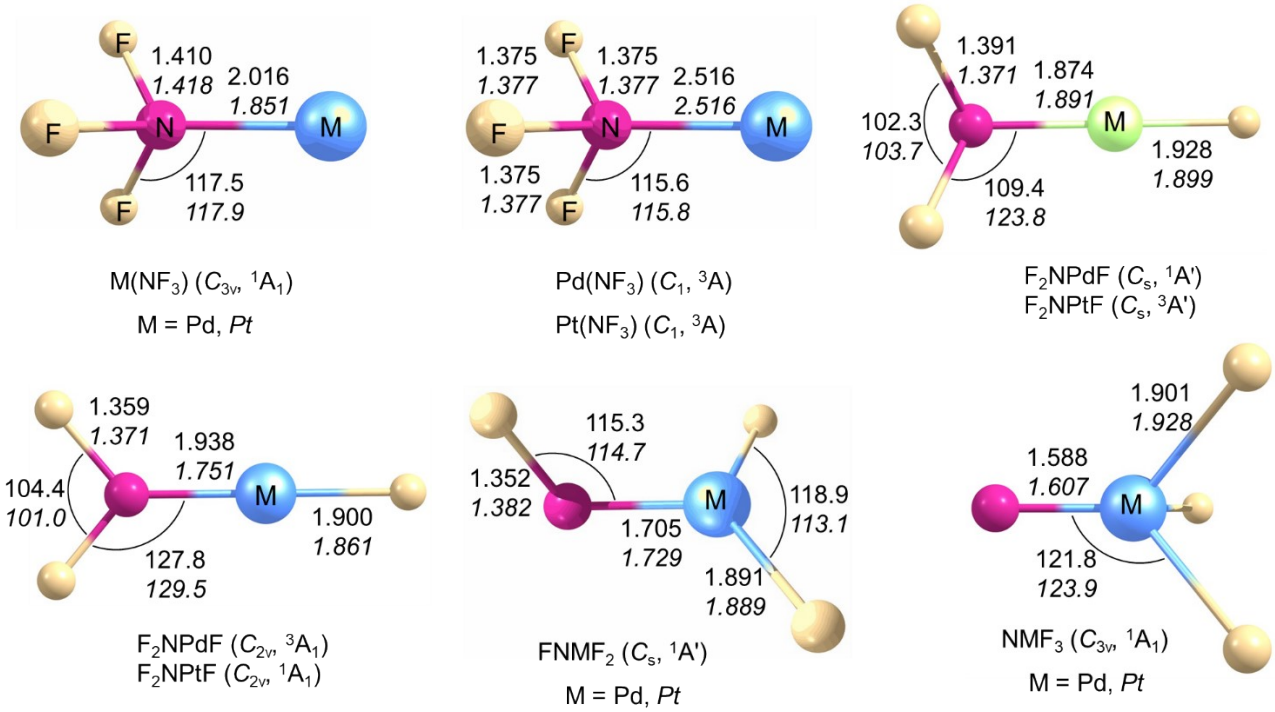

Fig. S8. Calculated geometries (bond lengths in angstroms and bond angles in degrees) of $M(NF_3)$, F_2NPtF, $FNPtF_2$ and NMF_3 (M = Pd, Pt) at B3LYP/aug-cc-pVTZ-(PP) level of theory.

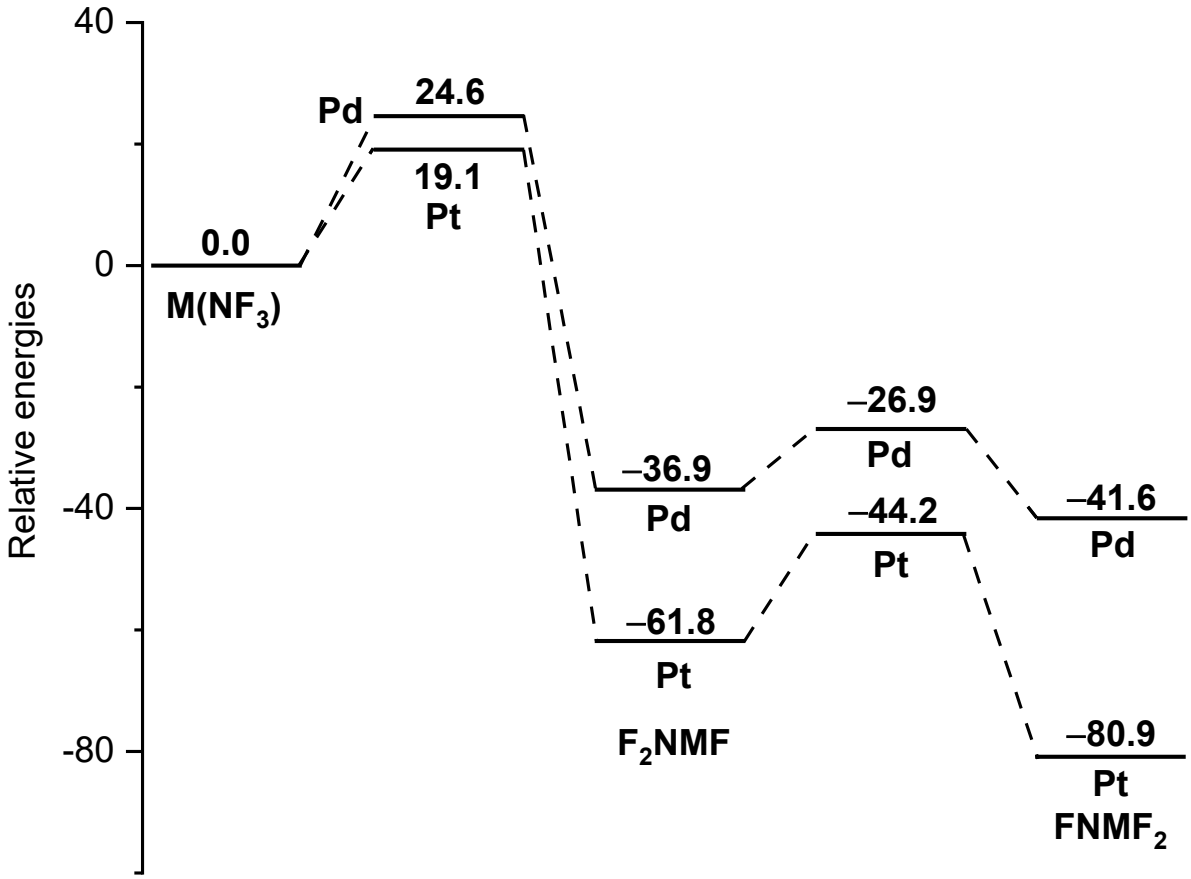

Fig. S9. The singlet potential energy profile of the isomeric reaction of $M(NF_3)$ to $FNMF_2$ (M = Pd, Pt) at the CCSD(T)/aug-cc-pVTZ(-PP)//B3LYP/aug-cc-pVTZ(-PP) level of theory. The energies are in kcal/mol.

Table S1 Calculated vibrational frequencies (in cm^{-1}) and IR intensities (in km/mol) of the NF_3Pd isomers in the electronic ground state at the B3LYP/aug-cc-pVTZ(-PP) and CCSD(T)/aug-cc-pVTZ(-PP) levels.

Complex	B3LYP		CCSD(T)
	ν	I	ν
$Pd(NF_3)$ (C_{3v}, $^1A_1$)	849	731	878
	703	159	813
	703	159	813
	610	11	629
	445	10	475
	445	10	475
	217	10	176
	155	3	159
	155	3	157
F_2NPdF (C_{2v}, $^3A_1$)	1075	410	–
	946	173	–
	608	92	–
	580	50	–
	284	1	–
	263	3	–
	245	2	–
	108	7	–
	55	7	–
$FNPdF_2$ (C_s, $^1A'$)	994	232	–
	820	60	–
	610	104	–
	579	94	–
	319	0.5	–
	310	0.4	–
	152	12	–
	101	1	–
	92	10	–
$NPdF_3$ (C_{3v}, $^1A_1$)	1106	65	1075
	608	52	594
	567	66	549
	567	66	549
	275	3	243
	275	3	242
	197	7	183
	107	1	91
	107	1	83

Table S2 Calculated vibrational frequencies (in cm^{-1}) and IR intensities (in km/mol) of the NF_3Pt isomers in the electronic ground state at the B3LYP/aug-cc-pVTZ-PP and CCSD(T)/aug-cc-pVTZ(-PP) levels.

Complex	B3LYP		CCSD(T)
	ν	I	ν
$Pt(NF_3)$ (C_{3v}, $^1A_1$)	901	811	854
	667	121	750
	667	121	750
	624	42	634
	452	13	476
	452	13	476
	296	0.2	269
	244	6	248
	244	6	247
F_2NPtF (C_{2v}, $^1A_1$)	1064	395	1056
	808	183	835
	666	137	667
	635	0.6	628
	494	0.2	491
	394	6	388
	375	0.5	376
	146	2	150
	47	3	66
$FNPtF_2$ (C_s, $^1A'$)	925	160	933
	833	119	804
	640	109	608
	608	79	578
	353	1	344
	298	0.3	294
	184	5	194
	123	4	157
	113	0.4	144
$NPtF_3$ (C_{3v}, $^1A_1$)	1175	61	1148
	617	52	616
	553	66	559
	553	66	558
	268	4	260
	268	4	259
	204	6	210
	50	2	93
	50	2	90

Table S3. The relative energies (kcal/mol) of different isomers of F_3NM (M = Pd, Pt) at B3LYP/aug-cc-pVTZ(-PP) and CCSD(T)/aug-cc-pVTZ(-PP) levels.

Species	Methods	
	B3LYP/aug-cc-pVTZ(-PP)	CCSD(T)/aug-cc-pVTZ(-PP)
$Pd(NF_3)$ (C_{3v}, $^1A_1$)	0.0	0.0
$Pd(NF_3)$ (C_s, $^3A'$)	26.0	33.0[a]
F_2NPdF (C_s, $^1A'$)	–30.4	–28.7[a]
F_2NPdF (C_{2v}, $^3A_1$)	–39.2	–36.9[a]
$FNPdF_2$ (C_s, $^1A'$)	–46.3	–41.6[a]
$NPdF_3$ (C_{3v}, $^1A_1$)	–8.4	–4.5
$Pt(NF_3)$ (C_{3v}, $^1A_1$)	0.0	0.0
$Pt(NF_3)$ (C_1, ^3A)	20.1	25.1[a]
F_2NPtF (C_{2v}, $^1A_1$)	–62.8	–61.7
F_2NPtF (C_s, $^3A'$)	–50.3	–40.9[a]
$FNPtF_2$ (C_s, $^1A'$)	–82.4	–80.9
$NPtF_3$ (C_{3v}, $^1A_1$)	–62.8	–61.7

[a] The single point energy obtained at CCSD(T)/aug-cc-pVTZ(-PP) level using the DFT (B3LYP/aug-cc-pVTZ(-PP)) geometries.

Table S4. The Cartesian coordinates of the studied complexes at the B3LYP/aug-cc-pVTZ(-PP) level.

$Pd(NF_3)$ (C_{3v}, $^1A_1$) **A**			
E = -481.734279 au			
0 1			
N	0.00000000	0.00000000	-0.93896700
F	0.00000000	1.25041300	-1.59113900
F	1.08289000	-0.62520700	-1.59113900
F	-1.08289000	-0.62520700	-1.59113900
Pd	0.00000000	0.00000000	1.07681600

$Pd(NF_3)$ (C_s, $^3A'$)			
E = -481.692849 au			
0 3			
N	1.24525100	0.00013200	-0.00026000
F	1.84190600	-0.24781800	-1.21386600
F	1.84175900	1.17515200	0.39281000
F	1.84018200	-0.92787600	0.82169300
Pd	-1.27024700	0.00008600	-0.00008500
F_2NPdF (C_s, $^1A'$)			
E = -481.794501 au			
0 1			
F	-0.01322600	-1.95104700	1.08294100
F	-0.01322600	-1.95104700	-1.08294100
F	0.54458600	2.34607600	0.00000000
N	-0.57925500	-1.28657600	0.00000000
Pd	-0.01322600	0.50022200	0.00000000
F_2NPdF (C_{2v}, $^3A_1$)			
E = -481.796799 au			
0 3			
F	0.00000000	1.07368700	-2.19148800
F	0.00000000	-1.07368700	-2.19148800
F	0.00000000	0.00000000	2.47803500
N	0.00000000	0.00000000	-1.35871700
Pd	0.00000000	0.00000000	0.57946700
$FNPdF_2$ (C_s, $^1A'$) **C**			
E = -481.808146 au			
0 1			
F	-0.32942800	-2.31960700	0.00000000
F	-0.32942800	1.09636500	1.62824400
F	-0.32942800	1.09636500	-1.62824400
N	0.64265900	-1.37965800	0.00000000
Pd	0.09556400	0.23477200	0.00000000

$NPdF_3$ (C_{3v}, $^1A_1$)			
E = -481.747617 au			
0 1			
F	0.00000000	1.61608800	0.80217600
F	-1.39957300	-0.80804400	0.80217600
F	1.39957300	-0.80804400	0.80217600
N	0.00000000	0.00000000	-1.78726900
Pd	0.00000000	0.00000000	-0.19886700
$Pt(NF_3)$ (C_{3v}, $^1A_1$) **B**			
E = -473.680463 au			
0 1			
N	0.00000000	0.00000000	-1.12874700
Pt	0.00000000	0.00000000	0.72196400
F	0.00000000	1.25317100	-1.79303500
F	1.08527800	-0.62658600	-1.79303500
F	-1.08527800	-0.62658600	-1.79303500
$Pt(NF_3)$ (C_1, ^3A)			
E = -473.648403 au			
0 3			
N	-1.60823200	-0.00038800	-0.00069700
Pt	0.90833500	-0.00008600	-0.00018000
F	-2.21006400	-0.86652400	-0.88460000
F	-2.20480700	-0.33291900	1.19407400
F	-2.20651700	1.20049000	-0.30737200
F_2NPtF (C_{2v}, $^1A_1$)			
E = -473.780510 au			
0 1			
F	0.00000000	1.05777300	-2.24171900
F	0.00000000	-1.05777300	-2.24171900
F	0.00000000	0.00000000	2.24241400
N	0.00000000	0.00000000	-1.36990900
Pt	0.00000000	0.00000000	0.38152000

F_2NPtF (C_s, $^3A'$)

E = -473.760638 au

0 3

F	-2.28024900	-1.07727900	-0.10714700
F	-2.27904000	1.07831200	-0.10689400
F	2.28647900	0.00066600	-0.15325500
N	-1.48743600	-0.00013700	0.19313000
Pt	0.39573500	-0.00018400	0.02504800

$FNPtF_2$ (C_s, $^1A'$) **D**

E = -473.811750 au

0 1

F	-0.28154600	-2.40147700	0.00000000
F	-0.28154600	0.87284000	1.73674100
F	-0.28154600	0.87284000	-1.73674100
N	0.67530500	-1.40481800	0.00000000
Pt	0.03685400	0.20174200	0.00000000

$NPtF_3$ (C_{3v}, $^1A_1$)

E = -473.780477 au

0 1

F	0.00000000	1.60006300	0.91705500
F	-1.38569500	-0.80003200	0.91705500
F	1.38569500	-0.80003200	0.91705500
N	0.00000000	0.00000000	-1.76582900
Pt	0.00000000	0.00000000	-0.15897000

TS: $F_3NPd \rightarrow F_2NPdF$

E = -481.698881 au

0 1

N	-0.98689100	-0.06962300	-0.11114100
F	-0.77270500	1.83630200	-0.42516400
F	-1.73756600	-1.12813600	-0.70982800
F	-1.58227100	-0.01072300	1.10875600
Pd	0.95089400	-0.12586100	0.02204600

TS: $F_2NPdF \rightarrow FNPdF_2$			
E = -481.781959 au			
0 1			
F	-1.80026800	-0.93524200	-0.16638500
F	-1.76854600	1.25411200	-0.18929800
F	2.26205500	0.52428600	-0.02621900
N	-1.28707500	0.20039500	0.55274700
Pd	0.45153000	-0.19546000	-0.00939400
TS: $F_3NPt \rightarrow F_2NPtF$			
E = -473.636907 au			
0 1			
N	1.19682100	-0.08970100	0.06049200
Pt	-0.65612500	-0.07392200	-0.01705500
F	0.99507100	1.90623900	0.34797800
F	1.86256100	-1.01427600	0.85851000
F	1.89792300	-0.18153800	-1.10572500
TS: $F_2NPtF \rightarrow FNPdF_2$			
E = -473.757370 au			
0 1			
F	-1.58771100	-1.13019600	-0.07406400
F	-1.94956800	1.26286600	-0.26032000
F	1.94900900	0.76165600	0.02283500
N	-1.31766400	0.43450900	0.60629600
Pt	0.30151400	-0.14218600	-0.01846300

Table S5. The Cartesian coordinates of the studied complexes at the CCSD(T)/aug-cc-pVTZ(-PP) level.

$Pd(NF_3)$ (C_{3v}, $^1A_1$) **A**			
E = -480.70740949 au			
0 1			
N	0.00000	0.00000	-0.97592
F	0.00000	1.24374	-1.61545
F	1.07711	-0.62187	-1.61545
F	-1.07711	-0.62187	-1.61545

Pd 0.00000 0.00000 1.09671
$NPdF_3$ (C_{3v}, $^1A_1$) E = -480.71462197 au 0 1 F 0.00000 1.61609 0.80218 F -1.39957 -0.80804 0.80218 F 1.39957 -0.80804 0.80218 N 0.00000 0.00000 -1.78727 Pd 0.00000 0.00000 -0.19887
$Pt(NF_3)$ (C_{3v}, $^1A_1$) **B** E = -472.59408358 au 0 1 N 0.00000 0.00000 -1.15499 Pt 0.00000 0.00000 0.73025 F 0.00000 1.24698 -1.81018 F 1.07991 -0.62349 -1.81018 F -1.07991 -0.62349 -1.81018
F_2NPtF (C_{2v}, $^1A_1$) E = -472.69250077 au 0 1 F 0.00000 1.05777 -2.24172 F 0.00000 -1.05777 -2.24172 F 0.00000 0.00000 2.24241 N 0.00000 0.00000 -1.36991 Pt 0.00000 0.00000 0.38152

F_2NPtF (C_s, $^1A'$)

$FNPtF_2$ (C_s, $^1A'$) **D**

E = -472.72305132 au

0 1

F	-0.28096	-2.39978	0.00000
F	-0.28096	0.85666	1.76885
F	-0.28096	0.85666	-1.76885
N	0.66821	-1.41877	0.00000
Pt	0.03729	0.20653	0.00000

$NPtF_3$ (C_{3v}, $^1A_1$)

E = -472.69260045 au

0 1

F	0.00000	1.60006	0.91705
F	-1.38569	-0.80003	0.91705
F	1.38569	-0.80003	0.91705
N	0.00000	0.00000	-1.76583
Pt	0.00000	0.00000	-0.15897